

STEPAN SPATENKA¹
VLASTIMIL FILA¹
BOHUMIL BERNAUER¹
JOSEF FULEM¹
GABRIELE GERMANI²
YVES SCHUURMAN²

¹Institute of Chemical
Technology, Technicka 5,
Prague 6, Czech Republic

²Institute de recherches sur
la Catalyse – CNRS,
Villeurbanne, France

SCIENTIFIC PAPER

66.011 +66.097:66.023

MODELLING AND SIMULATION OF MICROCHANNEL CATALYTIC WGS REACTOR FOR AN AUTOMOTIVE FUEL PROCESSOR

The water–gas shift (WGS) is one of the major steps for H₂ production from gaseous, liquid and solid hydrocarbons. It is used to produce hydrogen for ammonia synthesis, to adjust the hydrogen–to–carbon monoxide ratio of synthesis gas, to detoxify gases. The WGS reactor is widely used as a part of fuel processors which produce hydrogen–rich stream from hydrocarbon–based fuels in a multi–step process. The WGS unit is placed downstream the fuel reformer in order to increase overall efficiency of hydrogen production and to lower CO content in reformat. Fuel processors stand for considerable option for fuelling PEM fuel cells for both portable and stationary applications. Micro–structured reactors are used with benefits of process miniaturization, intensification and higher heat and mass transfer rates compared with conventional reactors. Micro–structured reactor systems are essential for processes where potential for considerable heat transfer exists as well as for kinetic studies of highly exothermic reactions at near–isothermal conditions. Modelling and simulation of a microchannel reactor for the WGS reaction is presented. The mathematical models concern a single reaction channel with porous layer of catalyst deposited on the metallic wall of the microstructure unit. Simplified one–phase and more sophisticated two–phase models, with separate mass and energy balances for gas and solid phase at different levels of complexity, were developed. The models were implemented into gPROMS process modelling software. The models were used for an estimation of parameters in a kinetic expression using experimental data obtained with a new WGS catalyst. The simulations provide detailed information about the composition and temperature distribution in gas phase and solid catalyst inside the channel.

Key words: water–gas shift, catalyst, microchannel, reactor, fuel processor, modelling.

Fuel cell power systems for transportation application or mobile source of electrical energy have received increased attention in recent years because of their potential for high fuel efficiency and lower emissions [1]. A fuel cell converts hydrogen and oxygen into water, directly generating electrical energy from chemical energy without being restricted by efficiency limits of Carnot thermal cycle [2]. The most promising fuel–cell technology for transportation applications has been shown to be the polymer electrolyte membrane (PEM) fuel cell operating with hydrogen [3]. Lacking a hydrogen fuel delivery system, a fuel processor (FP) may be required to generate a hydrogen–rich stream using infrastructure fuels as gasoline or diesel [4]. The most efficient fuel–cell anodes are based on precious metals [5] which are sensitive to deactivation by carbon monoxide adsorption at low temperatures and it is essential to reduce the amount of CO entering the cell.

The fuel processor (FP) produces hydrogen–rich streams from hydrocarbon–based feedstocks in a multi–step process [6]. Vaporized fuel is converted in a reforming unit that involves steam reforming (feed is composed of fuel and steam), or autothermal reforming (i.e. feed is fuel, steam, and air). Although the specific

composition of the reformer effluent depends on the reforming technology and choice of operating conditions, we have to take into account the presence of CO in concentration of about 8–10 % mol. Because CO is a poison to the fuel cell electrocatalyst, its presence in the product stream must be reduced to less than 50 ppm. This task is partially accomplished by a water–gas shift (WGS) reactor. WGS is typically performed as a staged process. Conversion of CO from reforming requires high temperature shift (HTS) run at close to equilibrium to reduce the levels to 3–5% CO. Then, medium temperature shift (MDS) or/and low temperature shift (LTS) are used for further CO conversion and additional H₂ formation. Chemical equilibrium limits the conversion achieved in the WGS reactor, thus final CO cleanup occurs in the preferential oxidation unit (PrOx) in which the desired reaction is the oxidation of carbon monoxide [7, 8]. A schematic drawing of the overall FP system is shown in Fig. 1.

WGS is one of the major steps for H₂ production from gaseous, liquid and solid hydrocarbons. It is used to produce hydrogen for ammonia synthesis, to adjust the hydrogen–to–carbon monoxide ratio of synthesis gas, to detoxify gases. WGS reaction can take place whenever carbon monoxide and water are present and therefore it may be an important step or side reaction in many processes. In the fuel processor for PEM fuel cells, the WGS reactor provides primary CO cleanup, as well as secondary hydrogen production. The WGS is equilibrium exothermic reaction:

Author address: V. Fila, Institute of Chemical Technology, Technicka 5, 16628 Prague 6, Czech Republic
E-mail: vlastimil.fila@vscht.cz
Paper received and accepted: May 3, 2005

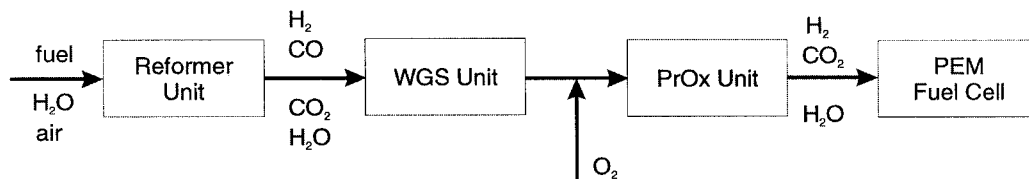


Figure 1. Schematic drawing of a fuel processing system



$$\Delta H_{298} = -41,09 \text{ kJmol}^{-1}$$

Typical commercially used catalysts for the reaction are $\text{Fe}_3\text{O}_4\text{-Cr}_2\text{O}_3$, used at 320–450°C as the high-temperature WGS catalyst, $\text{Cu-ZnO/Al}_2\text{O}_3$, which is the low temperature WGS catalyst used at 200–250°C, and $\text{Co-Mo/Al}_2\text{O}_3$, used at 150–400°C, which is stable towards sulphur impurities [9].

Kinetics of the WGS reaction on these commercial catalysts has been studied widely during past 50 years. However, there is still some disagreement on the precise form of the rate equation and values of rate constants and activation energies. The reaction kinetics for WGS reaction under high and low temperature conditions and for a wide variety of catalyst has been studied by Keiski and co-workers [9–11]. Apart from a number of kinetic expressions based on mechanisms, the following power-law type rate expression was found as appropriate for both low and high temperature catalysts [11]:

$$r_{\text{CO}} = k_0 \exp(-E/RT) c(\text{CO})^n c(\text{H}_2\text{O})^m (1 - \beta) \quad (2)$$

where β stands for the reversibility factor:

$$\beta = \frac{p(\text{CO}_2)p(\text{H}_2)}{p(\text{H}_2\text{O})p(\text{CO})K_{\text{eq}}} \quad (3)$$

and K_{eq} is the equilibrium constant of the reaction. More recently, Choi and Stenger [12] examined behaviour of commercial $\text{Cu/ZnO/Al}_2\text{O}_3$ catalyst between 120 and 250°C in a micro-reactor testing unit for using in fuel processor for FC application. Apart from several kinetic expressions based on reaction mechanism, a simple order reversible reaction rate equation (equation with $n = m = 1$) was found to fit their experimental data with a high degree of accuracy.

The activity of existing commercial WGS catalysts is generally low, and as a result, the largest fraction of the FP volume is occupied by WGS part [6]. Low-temperature catalyst activity and stability are the main issues related to the WGS reactor. Most industrial WGS catalysts have been developed for operation at higher temperatures. A viable WGS catalyst for an automotive fuel processor must demonstrate sufficient activity over a reasonable temperature range, have 2000–5000 h stability, be non-pyrophoric (a feature not possessed by conventional Cu-based catalysts), and have quick start-up procedure [8]. There has been considerable attention placed on new WGS catalysts for

fuel processing applications. However, an effective commercial catalyst is still under development [13]. One catalyst receiving much attention as a potential candidate is cerium oxide or ceria (CeO_2) loaded with a reduction promoter metal, for example Rh, Pt, Pd, Ni, Fe, Co and Cu [13–16]. However, there is a disagreement on the reaction mechanism and role of ceria and promoters in the WGS mechanism.

Conventional fuel processing technology is based on fixed-bed reactors, which do not scale well with the small modular nature of fuel cells. The design of fuel processor based on micro-structured reactors could overcome this problem eventually. Tonkovich et al. [17] reported on a different approach to WGS using microchannel reactors. More recently, the utilization of microreactors for the gas phase reactions and for portable hydrogen production is excellently reviewed by Kolb and Hessel [18] and by Holladay et al. [19]. Microchannel reactors reduce size of conventional chemical reactors without lowering the throughput. Heat and mass transport limitations slow the observed reaction rates in conventional reactors, but are reduced in microchannel reactors, and thus facilitate exploiting fast intrinsic reaction kinetics, i.e. high effectiveness factor. For these reasons, microchannel reactors find usage in fuel processors, which are a critical reactor technology for the deployment of PEM-based fuel cells for both portable and stationary power application [1].

The aim of this work was to develop mathematical models of a microchannel catalytic reactor, to use them for estimation of kinetic parameters for experimental data from a test microreactor and finally to simulate the pilot plant or full-scale reactor. The mathematical models concern a single reaction channel with porous layer of catalyst deposited on the channel's wall. Channels are formed in metallic platelet which is a basic structural element of a microstructure unit. Simplified 1-dimensional and more detailed 2-dimensional 2-phase models, with separate mass and energy balances for gas and solid phase, were developed. The conventional empirical kinetic equation given in Eq. was used for processing experimental data from microchannel catalytic reactor coated by a new $\text{Pt/CeO}_2/\text{Al}_2\text{O}_3$ catalyst. Parameters of a kinetic expression for WGS reaction were estimated from experimental data using the 1-D model. Simulations and parameter estimation were performed in gPROMS modelling, simulation and optimization environment [20]. The gPROMS software permits mathematical modelling of arbitrarily complex dynamic operations

distributed over two spatial domains in terms of mixed systems of integral, partial differential, and algebraic equations. Results of the simulations provide detailed information about the composition and temperature distribution in gas phase and solid catalyst inside the channel.

MATHEMATICAL MODELS

There are several alternatives in modelling microchannel reactor systems with catalytic active layer. Two approaches are used in this study; they are called 1-D model and 2-D model. Both are 2-phase models with different heat balances for gas and solid phase; 2-D model (by contrast to 1-D model) considers 2-phases also in the mass balances. Microreactor built of microstructured metal alloy platelets with microchannels and catalytic layer deposited on the channel's wall is considered. The models differ mainly in character of catalytic layer by involving a radial concentration profile in the 2-D model. Description of the dynamic models is given hereinafter and the equations are summarized in the appendix. Dynamic models are presented in spite of usage of steady states in this study, because the dynamic simulations were performed to obtain a steady state due to convergence problems with stationary simulations.

Main assumptions

Some assumptions are the same for both models:

- *Single-channel model.* The flow distribution at the reactor inlet and outlet is supposed to be uniform as well as the temperature distribution in cross section area of the microreactor. Therefore, every channel within the microreactor structure behaves alike and only one channel needs to be analyzed. Fig. 2 shows scheme of the microstructured platelet and the particular

single-channel geometry used in this study. A cylindrical channel (half of it) is used to approximate the actual shape of the channel, together with the catalytic layer on the wall. The supporting metal alloy platelet is considered in the enthalpy balances.

- *Adiabatic channels.* The adiabatic behaviour of the reactor is considered.

- *Constant pressure.* No pressure drop is considered in this study.

- *Heat conducting walls.* Thermal conductivity of the high-conducting metallic plates cannot be neglected. The constant temperature in radial direction and developing axial temperature profile are considered.

- *No homogeneous chemical reactions take place.* The chemical reactions in the gas-phase are neglected.

- *Ideal gas behaviour.* The gas mixture is assumed ideal since pressure is usually low (<5 bar) and temperatures are elevated (200–350°C).

1-D model

The first model represents the 1-D plug-flow reactor model for the gas phase. If the gas-phase reactions are neglected, only the surface reaction needs to be considered and it is involved in the gas phase mass balance via the effectiveness factor of the catalytic layer (Eq. (7)). For the studied system, the metal alloy platelet and two enthalpy balances are considered (Appendix; Equations 10 and 13) to cover both the convective nature of the gas-phase and significant axial heat conduction behaviour of the metallic plate (and its dominant heat capacity which is important for dynamic simulations). The heat transfer coefficient is used to cover the heat transfer between the solid and the gas phase. Temperature of the catalytic layer is assumed to be equal to temperature of the metallic plate. The heat capacity of the solid phase is calculated as weighted sum of plate and catalyst heat

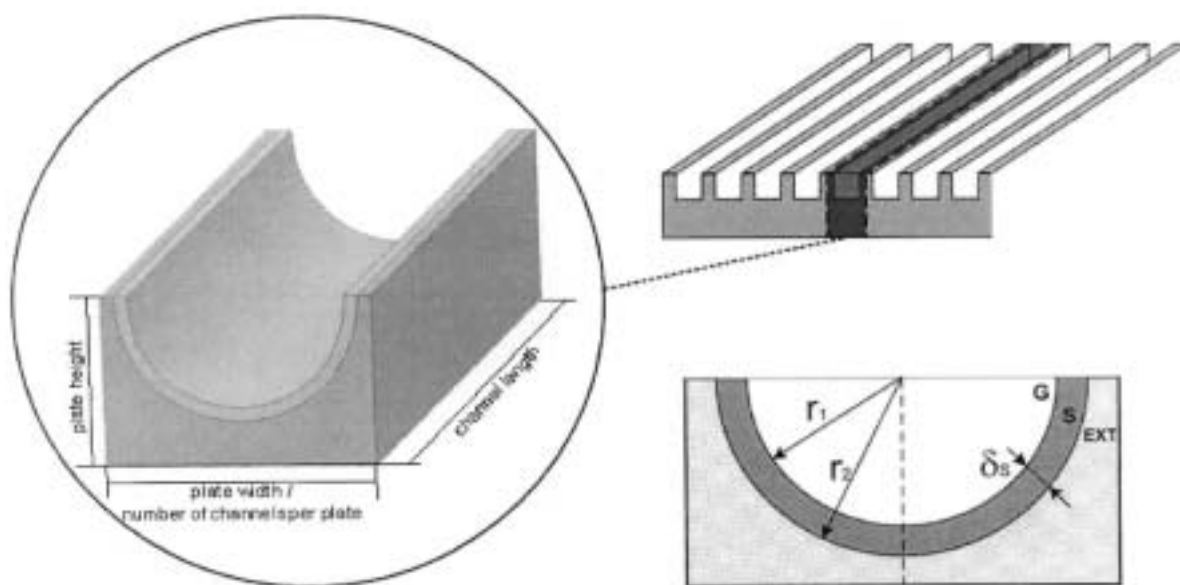


Figure 2. Scheme of the microchannel platelet, the channel detail and the channel cross-section area

capacity. The thermal conductivity of the metal alloy is taken as the dominant.

2-D model

The second modelling approach concerns the 2-D model. There are considered two-phases (gas and solid catalyst) described by 2 spatial dimensions – axial for the gas phase mass and heat balances and for the solid phase enthalpy balance, and radial for the solid phase mass balance. The axial convection, axial dispersion and the gas–solid phase mass transfer are taken into account in the gas–phase mass balance (Appendix; Eq. (16)). The solid–phase mass balance consists of radial diffusion term and the surface reaction term (Appendix; Eq. (20)). No axial diffusion is considered for the solid phase balance. The mass transport into the gas phase is covered by the boundary condition at the gas–solid phase interface using the gas–solid mass transfer coefficient (Appendix; Eq. (21)). The enthalpy balance for the gas phase takes into account axial heat conduction (Appendix; Eq. (24)). The constant temperature in radial direction due to high metal alloy thermal conductivity is considered for the solid phase (Appendix; Eq. (28)). The mean value of reaction rate for the calculation of heat generation in solid phase heat balance equation is used (Appendix; Eq. 29).

RESULTS AND DISCUSSION

WGS thermodynamics

The often-referred equilibrium constant of WGS reaction is given by Moe [21]:

$$\ln K_{eq} = \frac{A}{T} + B \quad (4)$$

where $A=4.577.8$ and $B=-4.33$. A conventional form of equilibrium constant calculated from thermodynamic properties can be represented by following equation:

$$\ln K_{eq} = \frac{a}{T} + b \cdot \ln T + c \cdot T + d \cdot T^2 + \frac{e}{T^2} + f \quad (5)$$

where the parameters can be found in literature [22]: $a = 5693.5$, $b = 1.077$, $c = 5.44 \times 10^{-4}$, $d = -1.125 \times 10^{-7}$, $e = -49170$ and $f = -13.148$.

The equilibrium constant of WGS reaction was calculated from thermodynamic properties of reaction components [23] in this work and we propose following parameters for equation : $a = 5729.8$, $b = 1.567$, $c = -1.512 \times 10^{-4}$, $d = 0$, $e = -47625$, $f = -16.006$. To simplify the calculation of the equilibrium constant the dependence of K_{eq} on temperature was fitted for the temperature range of 200–450°C by expression in the form of equation (4). We propose following values of parameters: $A = 4655.7$ and $B = -4.4022$. Based on the same thermodynamic data the temperature dependence of reaction enthalpy was calculated and the following equation was obtained when fitted by polynomial:

$$\Delta H = -43570 + 6.137 T + 2.602 \times 10^{-3} T^2 \text{ [J mol}^{-1}] \quad (6)$$

WGS kinetic parameters estimation using experimental data from microchannel test reactor

The experimental data from catalytic tests on WGS microreactor [24], were used for the kinetic parameter estimation. These data were obtained by experimental tests with new Pt/CeO₂/Al₂O₃ catalyst deposited on microchannels' wall. The test microreactor was made and provided by Institut für Mikrotechnik (IMM) Mainz and it consisted of microchannel platelets. The platelet is sketched in Fig. 2 and its main dimensions are summarized in Table 1. The experiments were performed isothermally and CO conversion at the end of reactor was measured for different temperatures and feed compositions.

Table 1. Dimensions of experimental microchannel platelet used in microreactor for kinetic tests

	mm
Channel width	0.6
Channel height	0.4
Plate height	1
Distance of channels	1
Length	50
Channels per plate	49

The mathematical model using the empirical exponential kinetic equation (Eq. 2) was applied in this work for fitting experimental data from microreactor with the new Pt/CeO₂/Al₂O₃ catalyst. Four parameters from Eq. (2) need to be estimated: k_0 , E , n and m . The parameters estimations (PE) were performed in gPROMS software. The objective function to be minimized is in the form of maximum likelihood estimation for a Gaussian distribution of measurement errors. The isothermal form of the 1D-model (PFR model) was used for the kinetic PE. The estimated parameters are summarized in Table 2. Comparisons of estimated conversions with the experimental ones are in Fig. 3. The quality of the fit is demonstrated in Fig. 4 by comparing the experimental and calculated CO conversions.

Table 2. Estimated kinetic parameters

$k_0 \text{ [(m}^3\text{)}^{n+m}\text{/kg/s/mol}^{n+m-1}]$	1.073×10^7
$E \text{ [kJ/mol]}$	73.211
$n \text{ [-]}$	0.178
$m \text{ [-]}$	0.638

Simulations with 2-D model

The estimated kinetic parameters were used for simulations performed with 2-D model. Mathematical model forms a system of algebraic and partial differential

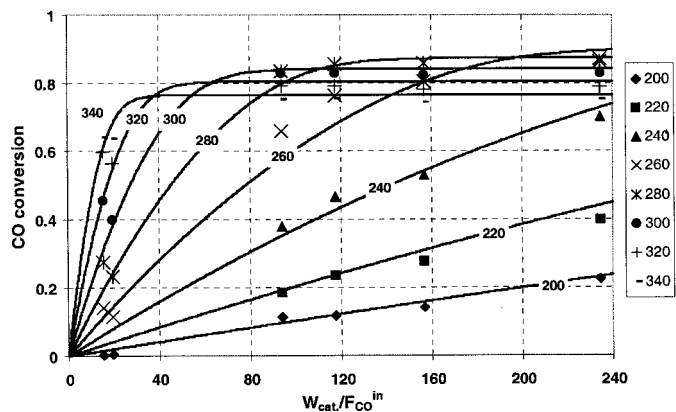


Figure 3. CO conversion as a function of $W_{cat.}/F_{CO}^{in}$ [kg.s/mol]. Comparison of experimental data for different temperatures (in °C) with predicted values

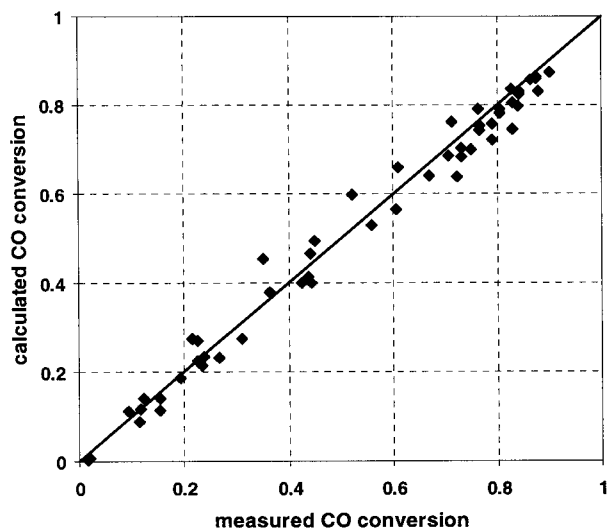


Figure 4. Parity plot – comparison of experimental CO conversion with calculated numerical value using 1-D model with estimated kinetics

equations. The solution of such system presents a considerable challenge for the accuracy and robustness of the numerical solution method used. The system of equations was solved in gPROMS simulation environment. In this work, only the steady state results are presented. However, the dynamic equations in form described in appendix were solved, because convergence problems occurred when trying to perform stationary simulations. The 1st or 2nd order backward finite difference method (BFDM) was used for axial coordinate discretization, while 2nd order orthogonal collocation on finite element method (OCFEM) was used for discretization in radial direction of the catalytic layer (for the 2-D model). The discretization of above models leads to system of differential and algebraic equation (DAE), which is solved by gPROMS using standard solver that implements fully-implicit Runge-Kutta method with a variable time step. Physicochemical properties of gas mixtures were calculated depending

on the actual temperature and composition using the MULTIFLASH databank [26] as a foreign object for gPROMS. Heat and mass transfer coefficients were calculated based on equations used in literature for modelling automotive catalytic converters [27].

Operation of WGS reactor (or reactors) in the fuel processor to generate fuel cell grade hydrogen rich stream must choose several operating parameters subject to several constraints. The main constraints include (i) inlet gas composition; (ii) inlet gas flow rate; (iii) the temperature exiting the reforming part of FP; (iv) CO concentration exiting the downstream processes; and (v) the water requirements for proper operation of fuel cell [12]. The gas composition is dependent on the fuel used in reforming stage and it is near equilibrium composition for the temperature at the reformer outlet. Due to high temperatures in the reformer (over 700°C) we have to consider CO content around 10 mol%. The inlet gas flow rate is constrained by catalyst activity and amount of catalyst in the microreactor. The flow rate should be low enough to achieve low CO concentration near the equilibrium conversion at the WGS reactor outlet. The CO concentration leaving the WGS reactors must be sufficiently low so it can be treated by preferential oxidation (about 1 mol%). The temperature of inlet gas can be in some range determined by heat management in the reforming part of fuel processor. Desired value is affected by activity of used catalyst in the first WGS step and we can consider values around 300°C. The minimum water content in the stream entering PEMFC should be near 12 mol% for proper humidification of a cell. We can suppose a sufficient access of water in the reforming, which positively affects the heat management and having positive effect on the equilibrium of the downstream WGS reaction and on its reaction rate. The value of $H_2O/CO = 3$ at the WGS inlet is used in this study.

The adiabatic WGS reactor operating with gas mixture containing 10 mol% CO, 10 mol% CO₂, 30 mol% H₂, 30 mol% H₂O and 20 mol% N₂ was simulated with the 2-D model for different inlet gas temperatures in the range 250–350°C. Results in the form of axial profiles of the gas temperature, CO and H₂ mole fractions and effectiveness factor of the catalytic layer are in the Fig. 5. Value of outlet temperature is indicated for each curve, since it mainly affects the gas composition at the reactor outlet. The adiabatic temperature rise in the reactor is in the range of 79–85°C for all the cases. The gas temperature affects the rate of CO consumption (H₂ generation). The effectiveness factor of the catalytic layer is calculated as ratio of integral mean reaction rate in the catalytic layer and the reaction rate at the gas phase –catalytic layer interphase ($r = 0$), usually referred as the internal effectiveness factor, that is not affected by the heat and mass transport from the gas phase to the catalyst. The values of the factor under 40% for higher temperatures indicate the importance of internal mass

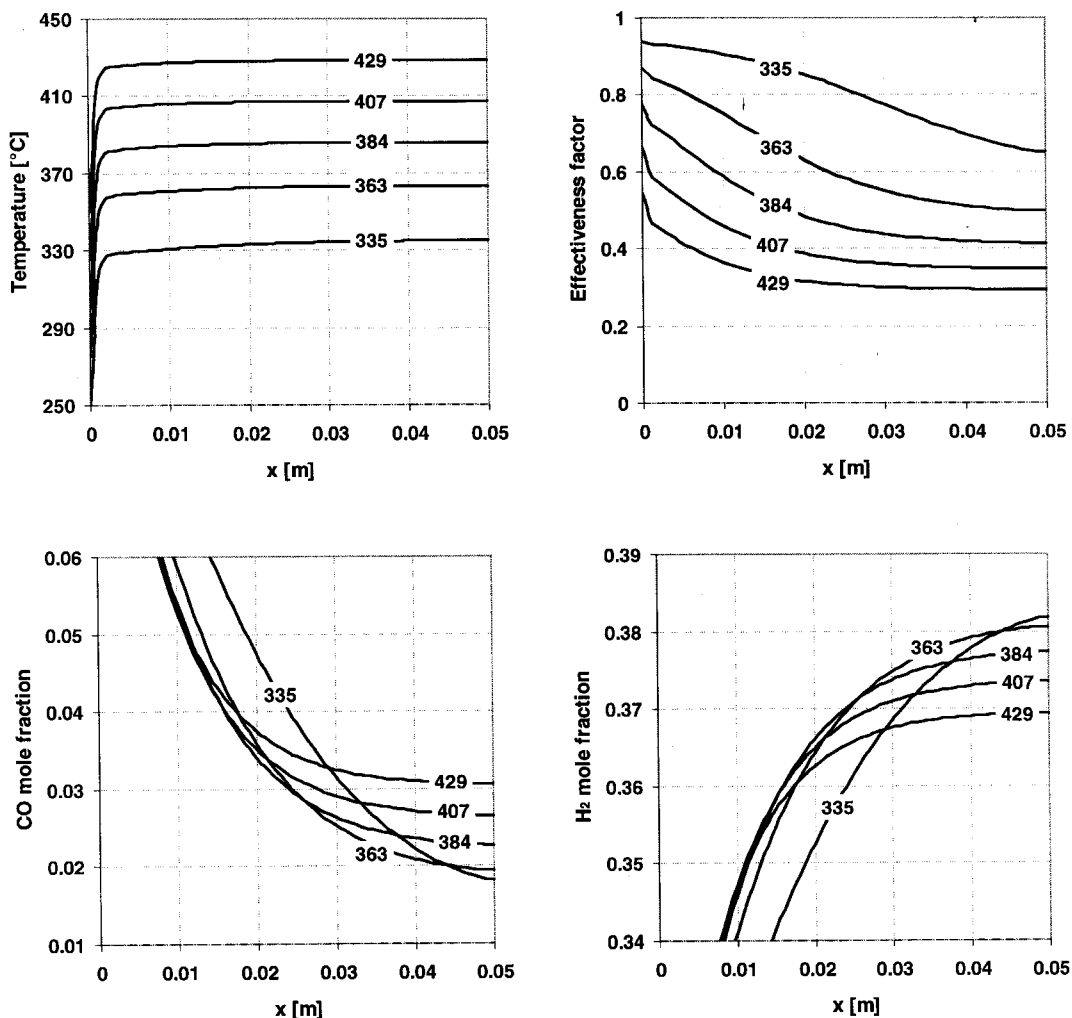


Figure 5. Simulation results of WGS reactor: axial profiles of the gas phase temperature, the effectiveness factor of the catalytic layer and CO and H₂ mole fraction. Curves are for different inlet gas temperatures 250, 275, 300, 325 and 350°C with corresponding outlet temperature (335, 364, 384, 407 and 429°C). Inlet composition: 10%CO, 10%CO₂, 30%H₂O, 30%H₂ and 20%N₂, $W_{\text{cat}}(\text{outlet})/F_{\text{CO}}(\text{inlet}) = 11.3 \text{ kg.s.mol}^{-1}$, pressure 3 bar

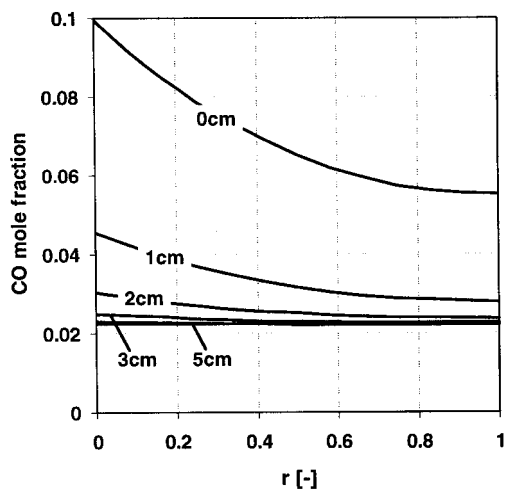


Figure 6. Simulation results of WGS reactor: radial profiles of CO mole fraction in the catalytic layer at different axial positions in the reactor – from the inlet (0 cm) to the outlet (5 cm). The inlet gas temperature is 300°C

transport limitations at higher reaction rates. The radial profiles of CO mole fraction at different axial positions for one case of the inlet temperature (300°C) are shown in Fig. 6. These results indicate that further improvement of textural characteristics of catalyst would be necessary in future research in this field.

CONCLUSIONS

Two mathematical models of microchannel reactor with catalytically active layer were described. The 1-D model was used for the estimation of kinetic parameters of the empirical kinetic expression by fitting experimental data from test microreactor coated with new Pt/CeO₂/Al₂O₃ WGS catalyst. The catalyst can be used in the WGS parts of fuel processors that generates hydrogen-rich stream for PEM fuel cell vehicle applications. The 2-D model was used for simulation of WGS microreactor operations providing detailed information about the composition and temperature

distribution in gas phase and solid catalyst inside the channel.

ACKNOWLEDGMENTS

This work was part of the Miniaturised Gasoline Fuel Processor for Fuel Cells Vehicle Application project (MINIREF) financed by the European Fifth Framework Programme. Authors greatly appreciate collaboration with all the partners in the project, mainly IRC-CNRS Villeurbanne, France, for the work on catalyst deposition and testing and IMM Mainz, Germany, for the microreactor manufacturing and providing.

Nomenclature

- A_M – cross-section area of the metallic platelet per channel
 β – reversibility factor
 c_i – mole concentration of specie i [mol/m³]
 c_P – specific heat capacity [J/kg/K]
 D_{eff}^G – dispersion coefficient [m²/s]
 D_{eff}^S – effective diffusion coefficient in the catalyst [m²/s]
 E – reaction activation energy [J/mol]
 ε – void fraction of the channel ($\varepsilon = r_1^2/r_2^2$)
 ε_s – porosity of the catalytic layer
 F^j – flow from the cell j [m³/s]
 ΔH – heat of reaction [J/mol]
 h – heat transfer coefficient [W/m²/K]
 η_S – effectiveness factor of the catalytic layer
 K_{eq} – equilibrium constant
 k_0 – reaction rate constant [(m³)^{n+m}/kg/s/mol^{n+m-1}]
 k_{Gi} – mass transfer coefficient for specie i [m/s]
 λ – thermal conductivity [J/s/m/K]
 L – length of the channel [m]
 N_{comp} – number of species
 NRS – number of reactions on the catalyst
 ν_{ik} – stoichiometric coefficient of specie i in the reaction k
 p_i – partial pressure of specie i [Pa]
 R^S – rate of the surface reaction [mol/m²cat./s]
 r – radial coordinate [m]
 r_1 – internal radius of the tube [m]
 r_2 – external radius of the tube [m]
 ρ_G – gas density [kg/m³]
 ρ_S – catalyst density [kg_{cat.}/m³cat.]
 S_G – the catalyst specific surface [m²/kg_{cat.}]
 T – temperature [K]
 t – time [s]
 v_z – linear velocity in axial direction [m/s]
 X – conversion
 z – axial coordinate [m]

Indexes:

- IN – reactor inlet
 i – component i
 G – gas phase
 S – solid phase (catalytic layer)
 M – metallic support
 MS – integrated balance of the catalytic layer and the metallic support

APPENDIX – MODEL EQUATIONS

Dynamic balance equations of both models presented in this work are summarized here.

1-D model

Mass balance:

for $i = 1$ to N_{comp} :

$$\varepsilon \frac{\delta c_i}{\delta t} = -\varepsilon v_z \frac{\delta c_i}{\delta z} + \eta_s (1 - \varepsilon) S_G (1 - \varepsilon_s) \rho_S \sum_{k=1}^{NRS} R_k^S \nu_{ik}^S \quad (7)$$

Boundary and initial conditions:

$$z = 0, c_i = c_i^{\text{IN}} \quad (8)$$

$$t = 0, c_i = c_i^0 \quad (9)$$

Enthalpy balance – gas phase:

$$c_{PG} \rho_G \frac{\delta T_G}{\delta t} = v_z c_{PG} \rho_G \frac{\delta T_G}{\delta z} + \frac{2}{r_1} h_{SG} (T_{MS} - T_G) \quad (10)$$

Boundary and initial conditions:

$$z = 0; T_G = T_G^{\text{IN}} \quad (11)$$

$$t = 0; T_G = T_G^0 \quad (12)$$

Enthalpy balance – solid phase:

$$\left(c_{PMPM} + \frac{\pi(r_2^2 - r_1^2)}{A_M} (1 - \varepsilon_s) C_{PS} \rho_S \right) \frac{\partial T_{MS}}{\partial t} = \lambda_M \frac{\delta^2 T_{MS}}{\delta z^2} + \frac{2\pi r_1}{A_M} h_{SG} (T_G - T_{MS}) + \frac{\pi(r_2^2 - r_1^2)}{A_M} \eta_S S_G (1 - \varepsilon_s) \rho_S \sum_{k=1}^{NRS} R_k^S (-\Delta H_k^S) \quad (13)$$

Boundary and initial conditions:

$$z = 0 \text{ and } z = L, \frac{\delta T_{MS}}{\delta z} = 0 \quad (14)$$

$$t = 0; T_{MS} = T_G^0 \quad (15)$$

2-D model

Mass balance – gas phase:

for $i = 1$ to N_{comp} :

$$\frac{\delta c_i^G}{\delta t} = D_{\text{eff}}^G \frac{\partial^2 c_i^G}{\partial z^2} - v_z \frac{\delta c_i^G}{\delta z} + \frac{2}{r_1} k_{Gi} ((c_i^S)_{r=r_1} - c_i^G) \quad (16)$$

Boundary and initial conditions:

$$z = 0; D_{\text{eff}}^G \frac{\delta c_i^G}{\delta z} = v_z (c_i^G - c_i^{G, \text{IN}}) \quad (17)$$

$$z = L; \frac{\delta c_i^G}{\delta z} = 0 \quad (18)$$

$$t = 0; c_i^G = c_i^{G,0} \quad (19)$$

Mass balance – solid phase:

for $i = 1$ to N_{comp} :

$$\varepsilon_s \frac{\delta c_i^s}{\delta t} = D_{i,eff}^s \left(\frac{\partial^2 c_i^s}{\partial r^2} + \frac{1}{r} \frac{\delta c_i^s}{\delta r} \right) + S_G (1 - \varepsilon_s) \rho_s \sum_{k=1}^{NBS} R_k^s v_{ik}^s \quad (20)$$

Boundary and initial conditions:

$$r = r_1; -D_{i,eff}^s \frac{\delta c_i^s}{\delta r} = k_{Gi} ((c_i^G)_{r=r_1} - c_i^s) \quad (21)$$

$$r = r_2; \frac{\delta c_i^s}{\delta r} = 0 \quad (22)$$

$$t = 0; c_i^s = c_i^{G,0} \quad (23)$$

Enthalpy balance – gas phase:

$$c_{PG} \rho_G \frac{\delta T_G}{\delta t} = \lambda_G^{eff} \frac{\partial^2 T_G}{\partial z^2} - v_z c_{PG} \rho_G \frac{\delta T_G}{\delta z} + \frac{2}{r_1} h_{SG} ((T_{MS})_{r=r_1} - T_G) \quad (24)$$

Boundary and initial conditions:

$$z = 0; \lambda_G^{eff} \frac{\delta T_G}{\delta z} = v_z c_{PG} \rho_G (T_G - T_G^N) \quad (25)$$

$$z = L; \frac{\delta T_G}{\delta z} = 0 \quad (26)$$

$$t = 0; T_G = T_G^0 \quad (27)$$

Enthalpy balance – solid phase:

$$\left(c_{PM} \rho_M + \frac{\pi(r_2^2 - r_1^2)}{A_M} (1 - \varepsilon_s) c_{PS} \rho_s \right) \frac{\partial T_{MS}}{\partial t} = \lambda_M \frac{\delta^2 T_{MS}}{\delta z^2} + \frac{2\pi r_1}{A_M} h_{SG} (T_G - T_{MS}) + \frac{\pi(r_2^2 - r_1^2)}{A_M} \eta_s S_G (1 - \varepsilon_s) \rho_s \sum_{k=1}^{NBS} R_k^s (-\Delta H_k^s) \quad (28)$$

where the mean reaction rate \bar{R}^s is defined as:

$$\bar{R}^s = \frac{2\pi}{\pi(r_2^2 - r_1^2)} \int_{r_1}^{r_2} r R^s (T_{MS}, c_i^s) dr \quad (29)$$

Boundary and initial conditions:

$$z = 0 \text{ and } z = L; \frac{\delta T_{MS}}{\delta z} = 0 \quad (30)$$

$$t = 0; T_{MS} = T_G^0 \quad (31)$$

REFERENCES

- [1] G. Hoogers, Fuel Cell Technology Handbook, CRC Press LLC, Boca Raton, 2003.

- [2] J. Larminie, A. Dicks, Fuel Cell Systems, Wiley, New York, 2000.
- [3] L. Carrette, K.A. Friedrich, U. Stimming, Fuel cells: Principles, types, fuels, and applications. ChemPhysChem. **1** (2000) 163–193.
- [4] M. Krumpelt, T.R. Krause, J.D. Carter, J.P. Kopasz, Fuel processing for fuel cell systems in transportation and portable power applications. Catalysis Today. **77** (2002) 3–16.
- [5] D.L. Trimm, Z.I. Onsan, Onboard fuel conversion for hydrogen–fuel–cell–driven vehicles. Catalysis Reviews – Science and Engineering. **43** (2001) 31–84.
- [6] C. Song, Fuel processing for low–temperature and high–temperature fuel cells: Challenges, and opportunities for sustainable development in the 21st century. Catalysis Today **77** (2002) 17–49.
- [7] T.V. Choudhary, D.W. Goodman, CO–free fuel processing for fuel cell applications. Catalysis Today. **77** (2002) 65–78.
- [8] J.M. Zalc, D.G. Löffler, Fuel processing for PEM fuel cells: transport and kinetic issues of system design, Journal of Power Sources **111** (2002) 58–64.
- [9] R.L. Keiski, T. Salmi, P. Niemistö, J. Ainassaari, Stationary and transient kinetics of the high temperature water–gas shift reaction. Applied Catalysis, A: General. **137** (1996) 349–370.
- [10] R.L. Keiski, T. Salmi, V.J. Pohjola, Development and verification of a simulation model for a non–isothermal water–gas shift reactor. The Chemical Engineering Journal. **48** (1992) 17–29.
- [11] R.L. Keiski, O. Desponds, Y.F. Chang, G.A. Somorjai, Kinetics of the water–gas shift reaction over several alkane activation and water–gas shift catalysts. Applied Catalysis, A: General. **101** (1993) 317–338.
- [12] Y. Choi, H.G. Stenger, Water gas shift reaction kinetics and reactor modeling for fuel cell grade hydrogen. Journal of Power Sources **124** (2003) 432–439.
- [13] G. Jacobs, L. Williams, U. Graham, G.A. Thomas, D.E. Sparks, B.H. Davis. Low temperature water–gas shift: in situ DRIFTS–reaction study of ceria surface area on the evolution of formates on Pt/CeO₂ fuel processing catalysts for fuel cell applications. Applied Catalysis A: General. **252** (2003) 107–118.
- [14] T. Bunluesin, R.J. Gorte, G.W. Graham, Studies of the water–gas–shift reaction on ceria–supported Pt, Pd, and Rh: Implications for oxygen–storage properties. Applied Catalysis B: Environmental. **15** (1998) 107–114.
- [15] S. Hilaire, X. Wang, T. Luo, R.J. Gorte, J. Wagner, A comparative study of water–gas–shift reaction over ceria–supported metallic catalysts. Applied Catalysis, A: General. **215** (2001) 271–278.
- [16] Q. Fu, S. Kudriavtseva, H. Saltsburg, M. Flytzani–Stephanopoulos, Gold–ceria catalysts for low–temperature water–gas shift reaction. Chemical Engineering Journal. **93** (2003) 41–53.
- [17] A.Y. Tonkovich, J.L. Zilka, M.J. LaMont, Y. Wang, Microchannel reactors for fuel processing applications. I. Water gas shift reactor. Chemical Engineering Science. **54** (1999) 2947–2951.
- [18] G. Kolb, V. Hessel, Micro–structured reactors for gas phase reactions. Chemical Engineering Journal **98** (2004) 1–38.
- [19] J.D. Holladay, Y. Wang, E. Jones, Review of Developments in Portable Hydrogen Production Using Microreactor Technology. Chemical Reviews **104** (2004) 4767–4789.
- [20] http://www.pcenterprise.com/products_gpoms.html.
- [21] J.M. Moe, Design of water–gas shift reactors. Chemical Engineering Progress. **58** (1962) 33–36.
- [22] G.C. Chinchen, P.J. Denny, J.R. Jennings, M.S. Spencer, K.C. Waugh, Synthesis of Methanol. Part 1. Catalysis and kinetics. Applied Catalysis **36** (1988) 1–65.

- [23] I. Barin, O. Knacke, O. Kubaschewski, Thermochemical properties of inorganic substances. Springer-Verlag, (1977).
- [24] G. Germani, Y. Schuurman, Unpublished data (2004).
- [25] gPROMS Advance User Guide, Release 2.2, Process System Enterprise Ltd., London, 2003.
- [26] <http://www.infochemuk.com>
- [27] T. Kirchner, G. Eigenberger, Optimization of the cold-start behaviour of automotive catalysts using an electrically heated pre-catalyst. Chemical Engineering Science, **51**(10) (1996) 2409-2418.



ŠTĚPÁN ŠPATENKA, PhD student

Štěpán Špatenka was born in 1978 in Prague, Czech Republic. After finishes his master's studies at Department of Organic technology at the Institute of Chemical Technology (ICT) in Prague in 2001, he started post-graduate studies in group of Prof. B. Bernauer at Department of Inorganic Technology at ICT Prague. He deals with mathematical modeling of catalytic and membrane processes, especially with catalytic microreactors.



VLASTIMIL FÍLA, Assistant Professor

Vlastimil Fíla was born in Czechoslovakia in 1968 and received his master degree (MSc) from Institute of Chemical Technology, Prague, in 1991. After his further education in the doctor course at the Department of inorganic technology at ICT Prague, he was appointed to a research associate at the same university in 1996 and received his doctor degree (PhD) in 1997. After one – year post – doctor studies at University Claude Bernard Lyon, France, he was promoted to assistant professor at ICT Prague in 1998. His current research interests are in chemical technology, reactor engineering, in organic membranes synthesis, membrane reactors and process modeling.



BOHUMIL BERNAUER, Associate Professor

Bohumil Bernauer was born in 1949 in Teplice, Czechoslovakia. He received his MSc. degree in 1972 and Ph.D. degree in 1978, both in Technical Chemistry at Faculty of Chemical Technology, Institute of Chemical Technology, Prague (ICTP). His main scientific interest focus on the reaction engineering of industrially important reactions, mass transfer in microporous membranes and mathematical modeling of chemical reactors. He is associated professor at Institute of Chemical Technology, Prague in the Department of Inorganic Technology and he is vice-rector for International Relations of ICTP.

He has spent 4 years at University Setif (Algeria) and 1 year at University Claude Bernard in Lyon (France) as visiting professor.

Professor Bernauer is a member of several scientific societies, such as European Membrane Society, Czech Society of Chemical Engineering. He is cooperating with partners from European Universities, research organizations and industrial sector in the frame of 5th and 6th FP of EU research projects.



JOSEF FULEM, PhD student

Josef Fulem was born in 1978 in Rokycany, Czech Republic. After finishes his master's studies at Department of Organic Technology at the Institute of Chemical Technology (ICT) in Prague in 2001, he started post-graduate study in group of Prof. B. Bernauer at Department of Inorganic Technology at ICT Prague. He deals with CFD simulations of catalytic and membrane processes. During the Ph.D. study he joined Ricardo, Inc. and his research interests are mainly in fuel cell systems.



GABRIEL GERMANI, PhD student

Born in Florence 1975, lived in the North of Italy (between Turin and Milan) until 1999.

1994 – 1999: Chemical engineering studies at Politecnico di Torino (PoliTo, Turin, Italy)

1999 – 2001: Spent two years in Sweden at Royal Institute of Technology (Kungl Teknisk Högskolan, KTH, Stockholm, Sweden) as an exchange student within the ERASMUS-TIME program.

2001: Obtained a double degree: M.Sc. in Chemical Engineering at PoliTo and KTH

Master work on onboard hydrogen production for fuel cell applications by partial oxidation of methanol over supported Pd catalysts

2002 – Present (May 2005): PhD work at Institut de Recherches sur la Catalyse (IRC, Lyon, France) within European project MINIREF: miniaturised gasoline fuel processor for fuel cell vehicle applications.



YVES SCHUURMAN, Researcher

Yves Schuurman was born in the Netherlands in 1964. He obtained his PhD degree at the Technical University of Eindhoven. He has been associate researcher at the Washington University in St Louis USA, before being appointed permanent researcher at the catalysis institute (IRC) in Lyon, France. His current research interests are in chemical kinetics, especially transient kinetics of heterogeneous catalysts.